



# Oxidovanadium(IV) sulfate-induced glucose uptake in HepG2 cells through IR/Akt pathway and hydroxyl radicals

Qian Zhao<sup>a</sup>, Deliang Chen<sup>a</sup>, Pingsheng Liu<sup>b</sup>, Taotao Wei<sup>b</sup>, Fang Zhang<sup>a,\*</sup>, Wenjun Ding<sup>a,\*\*</sup>

<sup>a</sup> Laboratory of Environment and Health, College of Life Sciences, University of Chinese Academy of Sciences, No. 19A YuQuan Road, Beijing 100049, China

<sup>b</sup> National Laboratory of Biomacromolecules, Institute of Biophysics, Chinese Academy of Sciences, 15 Datun Road, Beijing 100101, China

## ARTICLE INFO

### Article history:

Received 24 October 2014

Received in revised form 7 May 2015

Accepted 8 May 2015

Available online 15 May 2015

### Keywords:

Oxidovanadium(IV) sulfate

ROS

Glucose uptake

IR/Akt

HepG2 cells

## ABSTRACT

The insulin-mimetic and anti-diabetic properties of vanadium and related compounds have been well documented both *in vitro* and *in vivo*. However, the molecular basis of the link between vanadium and the insulin signaling pathway in diabetes mellitus is not fully described. We investigated the effects of reactive oxygen species (ROS) induced by oxidovanadium(IV) sulfate (VOSO<sub>4</sub>) on glucose uptake and the insulin signaling pathway in human hepatoma cell line HepG2. Exposure of cells to VOSO<sub>4</sub> (5–50 μM) resulted in an increase in glucose uptake, insulin receptor (IR) and protein kinase B (Akt) phosphorylation and intracellular ROS generation. Using Western blot, we found that catalase and sodium formate, but not superoxide dismutase, prevented the increase of hydroxyl radical ( $\cdot$ OH) generation and significantly decreased VOSO<sub>4</sub>-induced IR and Akt phosphorylation. These results suggest that VOSO<sub>4</sub>-induced  $\cdot$ OH radical, which is a signaling species, promotes glucose uptake via the IR/Akt signaling pathway.

© 2015 Elsevier Inc. All rights reserved.

## 1. Introduction

*In vitro* and *in vivo* studies have been demonstrated that vanadium compounds can improve glucose homeostasis and insulin resistance with their insulin-mimetic and anti-diabetic properties in type 1 and type 2 diabetes mellitus [1–4]. Vanadium and its compounds stimulate glucose transport and oxidation [5–7], and glycogen synthesis [8,9]. Moreover, some vanadium compounds have been previously documented to have insulin-like effects in streptozotocin (STZ)-diabetic rats [10]. Vanadium is known to accumulate in rat liver, an organ with many diabetes altered metabolic processes through the insulin signaling pathway [11,12]. In our previous studies, we also found that oral administration vanadium complexes enhance the glycogen synthesis and inhibit the gluconeogenesis by down-regulating the mRNA expression of phosphoenolpyruvate carboxykinase (PEPCK) in the liver of streptozotocin-induced diabetic rats [13,14]. However, the exact mechanism of the anti-diabetic activity of vanadium is not fully understood.

Several studies have demonstrated that V compounds with various oxidation states have different anti-diabetic effects [15–17]. The main oxidation states of vanadium under oxic conditions are V<sup>IV</sup>O<sup>2+</sup> and V<sup>V</sup>O<sup>3+</sup> [18]. In the various body fluids and cellular

compartments, the predominant species of vanadium will be vanadate(V). Vanadate(V) may enter cells by an anion transport system and be subsequently reduced by glutathione to oxidovanadium(IV) [18,19]. Vanadate(V) and oxidovanadium(IV) sulfate (VOSO<sub>4</sub>) are the main inorganic vanadium species relevant to intracellular function [10], which is likely to center on the regulation of reactive oxygen species (ROS) production and redox signaling [20]. Thus, interactions of vanadium compounds with cellular oxidation–reduction processes are important event in the anti-diabetic action of vanadium compounds [15]. Superoxide radicals (O<sub>2</sub><sup>•−</sup>), hydrogen peroxide (H<sub>2</sub>O<sub>2</sub>) and hydroxyl radicals ( $\cdot$ OH) are ubiquitous, highly reactive, short-lived product of oxygen metabolism that react with surrounding molecules at the site of formation [21]. Despite their potential for cytotoxicity, low levels of ROS are essential for the regulation of many biological functions and several biochemical processes, including intracellular messaging and cellular differentiation [22,23]. Recent studies have found that mitochondrial-derived ROS regulate protein tyrosine phosphatase (PTPase) oxidation, influencing growth factors signaling [24]. Hydroxyl radicals generated *in vivo* can act as physiological oxidizing agents for PTPase inactivation [25]. In addition, the serine/threonine kinase Akt occupies a central position in insulin signaling in that it is involved in stimulation of glucose uptake by insulin target cells [25–27]. It has been demonstrated that Akt is activated in a phosphatidylinositol 3-kinase (PI3K)-dependent manner by ROS and transition metal ions, such as Cu(II), Zn(II) and Ni(II) [26]. Regarding the signal-stimulating effects of ROS, redox-active transition metal ions capable of generating ROS in cells have been reported to stimulate Akt [28]. However, it

\* Corresponding author. Tel.: +86 10 8825 6079; fax: +86 10 8825 6460.

\*\* Corresponding author. Tel.: +86 10 8825 6290; fax: +86 10 8825 6460.

E-mail addresses: [zhangfang@ucas.ac.cn](mailto:zhangfang@ucas.ac.cn) (F. Zhang), [dingwj@ucas.ac.cn](mailto:dingwj@ucas.ac.cn) (W. Ding).

remains unclear whether an activation of Akt signaling by exposure of the insulin-sensitive cells to vanadium-induced ROS, be capable of eliciting the effects similar to those described above.

It has been demonstrated that oxidovanadium(IV) ions act peripherally, and that they rather than vanadate species are responsible for the insulin-like effects of vanadium [3]. Therefore, the aim of this study was to investigate the capability of  $\text{VOSO}_4$  stimulates Akt activity in cultured HepG2 cells, and to elucidate whether  $\text{VOSO}_4$ -induced Akt activation and glucose uptake are dependent of the formation of ROS.

## 2. Materials and methods

### 2.1. Reagents

$\text{VOSO}_4 \cdot 3.5\text{H}_2\text{O}$  was purchased from Aldrich Chemical Company (Milwaukee, WI, USA). Anti-phospho-Ser473 Akt, anti-Akt, anti-phospho-Tyr974 IR, anti-IR and anti- $\beta$ -actin antibodies were purchased from Cell Signaling Technologies (Beverly, MA, USA). Fetal bovine serum was purchased from Hyclone (UT, USA). Dulbecco's modified Eagle's medium (DMEM) was obtained from Invitrogen (CA, USA). 2',7'-dichlorodihydrofluorescein diacetate (DCFH-DA),  $\beta$ -nicotinamide adenine dinucleotide phosphate salt (NADPH), diphenylene iodonium (DPI), rotenone, catalase (CAT, 50,000 U/mg), superoxide dismutase (SOD, 3000 U/mg), and sodium formate were purchased from Sigma Chemical Co. (St. Louis, MO, USA). HEPES was purchased from Amresco Chemical Co. (OH, USA). Skim milk powder was obtained from BD (MD, USA). Enhanced chemiluminescence detection (ECL) reagent and ultra-pure water system were obtained from Millipore (MA, USA). 5,5-Dimethyl-1-pyrroline-N-oxide (DMPO) was purchased from Dojindo Molecular Technologies (Kumamoto-ken, Japan). D-[U- $^{14}\text{C}$ ]glucose was purchased from PerkinElmer Life Sciences (Mississauga, Ontario, Canada). 24-well plates and cell culture dishes were obtained from Costar Cambridge (MA, USA).

### 2.2. Cell culture

Human hepatocellular carcinoma (HepG2) cells were purchased from American Type Culture Collection (ATCC, Rockville, MD, USA), and were cultured in DMEM supplemented with 4.5 g/l glucose, 10% fetal bovine serum, 100 units/ml penicillin, and 100  $\mu\text{g}/\text{ml}$  streptomycin at 37 °C in 5%  $\text{CO}_2$ . All cell experiments were performed at 80 to 90% of cell confluence with viability  $\geq 90\%$  determined by the trypan blue staining. Cells were then harvested using 0.25% trypsin and sub-cultured into 60-mm culture dishes or 24-well plates according to selection of experiments.

### 2.3. Determination of glucose uptake

Glucose uptake assay were carried out according to the method of Tardif et al. [29] with modifications. In brief, on the day of the study, HepG2 cells were washed with 2 ml KRPH buffer (5 mM  $\text{Na}_2\text{HPO}_4$ , 20 mM HEPES, 1 mM  $\text{MgSO}_4$ , 1 mM  $\text{CaCl}_2$ , 136 mM NaCl, 4.7 mM KCl, and 0.2% BSA, pH 7.4). The cells were treated with 5, 10, 25 or 50  $\mu\text{M}$   $\text{VOSO}_4$  for 30 min, and then 1  $\mu\text{Ci}$  of D-[U- $^{14}\text{C}$ ]glucose was added to each well for 10 min. Glucose uptake was stopped by rising 3 times with ice-cold PBS. The cells were solubilized with 1% SDS at 37 °C for 10 min, and cell-associated radioactivity was analyzed by scintillation counting (1450 MicroBeta TriLux Microplate Scintillation and Luminescence Counter, PerkinElmer) according to the manufacturer's protocol. Glucose uptake was expressed as a fold of control. Nonspecific uptake ( $\leq 10\%$  of the total), determined in the presence of cytochalasin B (50  $\mu\text{M}$ ), was subtracted from the total uptake [30].

### 2.4. Immunoblot assay

Cells were plated in 60 mm culture dishes and treated with 5, 10, 25 and 50  $\mu\text{M}$   $\text{VOSO}_4$ . The cells were then lysed in radio immunoprecipitation assay (RIPA) buffer (150 mM NaCl, 100 mM Tris, 1% Triton X-100, 1% deoxycholic acid, 0.1% SDS, 5 mM EDTA, and 10 mM NaF, pH 8.0) supplemented with 1 mM phenylmethanesulfonyl fluoride (PMSF) on ice for 10 min. After centrifugation at 12,000 rpm for 15 min, the supernatant containing the total cellular protein extract was harvested and stored at  $-70$  °C prior to use. Total protein extracts were subsequently size-separated by SDS-PAGE, and transferred to a poly (vinylidene fluoride) (PVDF) membrane in 20 mM Tris-HCl (pH 8.0) containing 150 mM glycine and 20% (v/v) methanol. The membranes were blocked with 5% (m/v) skim dry milk for 1 h. The cells were incubated with the primary antibodies diluted (1:1000) against IR and Akt in Tris-buffered saline (20 mM Tris-HCl and 150 mM NaCl, pH 7.4) containing 0.1% Tween 20 (TBST) overnight at 4 °C and then incubated with the secondary antibody diluted (1:1000) at room temperature for 1 h. The membrane was washed with TBST three times for 5 min each. Immunoreactive bands were detected with enhanced chemiluminescence reagents according to the manufacturer's instructions.  $\beta$ -Actin was used as loading controls for the total protein content.

### 2.5. Detection of intracellular reactive oxygen species

DCFH-DA is widely used to detect the generation of ROS and for assessing the overall oxidative stress [31]. DCFH-DA as a molecular probe is able to diffuse through the cell membrane and become enzymatically hydrolysed by intracellular esterases to produce non-fluorescent DCFH. The oxidation of DCFH by intracellular ROS, mainly  $\text{H}_2\text{O}_2$ ,  $\cdot\text{OH}$  and other ROS, results in fluorescent DCF, which stains the cells [32]. In brief, HepG2 cells were cultured in 24-well plates at a density of  $1 \times 10^5$  cells/well. The cells were treated with 5, 10, 25 and 50  $\mu\text{M}$   $\text{VOSO}_4$  for 30 min. DCFH-DA (diluted with DMEM medium to final concentration of 10  $\mu\text{M}$ ) was applied to the cells and incubated for another 30 min at 37 °C. The cells were washed twice with ice-cold PBS and harvested for measurement of fluorescence intensity. DCF fluorescence intensity of each well was quantified using a fluorescence multi-well plate reader (TriStar LB941, Berthold, Germany) with excitation and emission wavelengths of 485 and 535 nm, respectively. Results were measured as mean fluorescence (arbitrary units, AU).

### 2.6. Electron spin resonance (ESR) measurement

ESR trapping technique, using DMPO as the spin trap, was employed to detect free radical generation. This technique involves the addition-type reaction of a short-lived radicals with a diamagnetic compound (spin trap) to form a relatively long-lived free radical product (spin adduct), which can be studied using conventional ESR. In this assay, the intensity of the spin adduct signal corresponds to the quantity of short-lived radicals trapped. The hyperfine couplings of the spin adduct are generally characteristic of the original trapped radicals [33]. ESR spectra were recorded on a Bruker ESP 300 spectrometer (Bruker, Ettlingen, Germany) and a flat cell assembly [33,34]. The reactants were mixed in a test tube in a final volume of 500  $\mu\text{l}$ . Hyperfine couplings were measured (up to 0.1 G) directly from the magnetic field separation using potassium tetraperoxochromate ( $\text{K}_3\text{CrO}_8$ ) and 1,1-diphenyl-2-picrylhydrazyl as reference standards. HepG2 cells ( $1 \times 10^7$ ) were mixed with 100 mM DMPO, 1 mM NADPH, 1 mM  $\text{VOSO}_4$ , and different ROS scavengers (20  $\mu\text{M}$  DPI, 50  $\mu\text{M}$  rotenone, 0.33 mg/ml SOD, 0.1 mg/ml CAT, or 300  $\mu\text{M}$  sodium formate). The reaction mixture was then transferred to a flat cell for ESR measurement.

## 2.7. Statistical analysis

All data are presented as mean  $\pm$  SEM of at least three independent experiments. Statistical analysis was performed with analysis of variance (ANOVA) for multiple comparisons, followed by a Fisher post hoc test. A value of  $P < 0.05$  was considered as statistically significant.

## 3. Results

### 3.1. VOSO<sub>4</sub> stimulates glucose uptake

To determine whether VOSO<sub>4</sub> could stimulate glucose uptake, HepG2 cells were treated with various concentrations of VOSO<sub>4</sub> for 30 min. As shown in Fig. 1, the levels of glucose uptake were induced by VOSO<sub>4</sub> in a dose-dependent manner. At 5, 10, 25 and 50  $\mu$ M, VOSO<sub>4</sub> induced a 1.3-, 1.6-, 1.9- and 1.6-fold stimulation in glucose uptake, respectively. The maximum level of glucose uptake was induced by 25  $\mu$ M VOSO<sub>4</sub>. These results indicate that within the concentration range, 5 to 50  $\mu$ M of VOSO<sub>4</sub> stimulates glucose uptake in HepG2 cells.

### 3.2. VOSO<sub>4</sub> increases IR/Akt phosphorylation

To further investigate if the observed glucose uptake induced by VOSO<sub>4</sub> was related to the insulin signaling pathway in HepG2 cells, the expressions of IR and Akt phosphorylation were measured by Western blot. Cells were incubated with the indicated VOSO<sub>4</sub> concentration for 30 min. The total cellular protein extracts were used to determine levels of phospho-IR for Tyr942 and IR protein as well as phospho-Akt for Ser473 and Akt proteins using immunoblot assay. As shown in Fig. 2, VOSO<sub>4</sub> significantly increased IR and Akt phosphorylation in a dose-dependent manner, whereas it did not alter the IR or Akt protein level. The induction of IR or Akt phosphorylation was maximum by the treatment of VOSO<sub>4</sub> at 25  $\mu$ M. These results suggest that VOSO<sub>4</sub> induced IR/Akt phosphorylation.

### 3.3. VOSO<sub>4</sub> increases ROS generation

Previous studies have demonstrated that ROS is involved in vanadium-induced biological activities [33,35]. If glucose uptake is responsible for some of the biological effects caused by vanadium, ROS generation may also play a role in VOSO<sub>4</sub>-induced stimulation in glucose uptake. To test this possibility, the ability of VOSO<sub>4</sub> to generate ROS in HepG2 cells was determined by dye staining and ESR. As

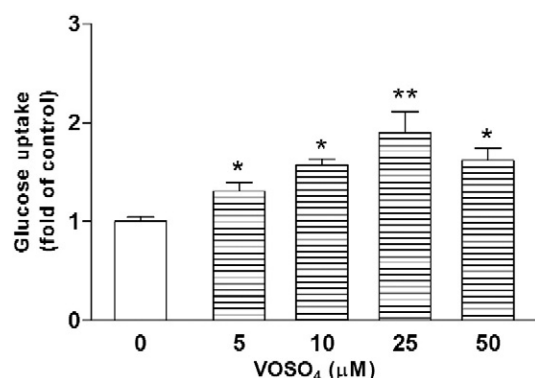


**Fig. 1.** Effects of VOSO<sub>4</sub> on glucose uptake in HepG2 cells. HepG2 cells were incubated with media containing 5, 10, 25 and 50  $\mu$ M of VOSO<sub>4</sub> for 30 min and then indicated with KRPH buffer containing 1  $\mu$ Ci of D-[U-<sup>14</sup>C] glucose for 10 min. Glucose uptake was determined in cells. Data are presented as mean  $\pm$  SEM of three independent experiments. \* $p < 0.05$ , \*\* $p < 0.01$  vs. the untreated control cells.

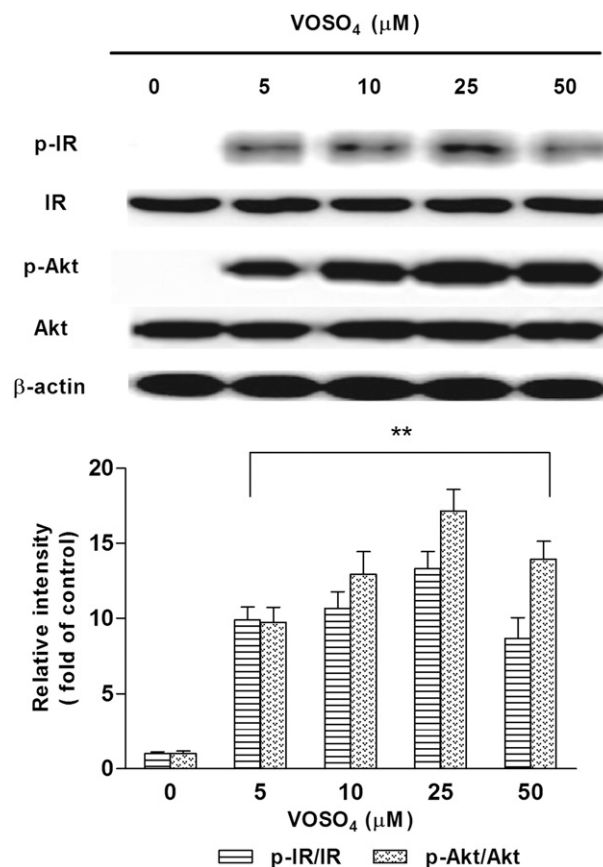


**Fig. 2.** Effects of VOSO<sub>4</sub> on phosphorylation of IR and Akt in HepG2 cells. HepG2 cells were treated with 5, 10, 25 and 50  $\mu$ M of VOSO<sub>4</sub> for 30 min. The total cellular protein extracts were prepared and subjected to immunoblot assay with antibodies against phospho-IR (Tyr942) and phospho-Akt (Ser473). The immunoblot signals quantified using ImageJ software are shown in the bar graph. The mean densitometry data from three independent experiments (one of which is shown here) were normalized to the result obtained in cells in the absence of VOSO<sub>4</sub> (control). Data are presented as mean  $\pm$  SEM of three independent experiments. \*\* $p < 0.01$  vs. the untreated control cells.

shown in Fig. 3, in the presence of 25 or 50  $\mu$ M VOSO<sub>4</sub>, ROS generation, as measured by increased DCF fluorescence, was increased approximately 1.5-fold in vanadium-treated, compared with untreated control, HepG2 cells.

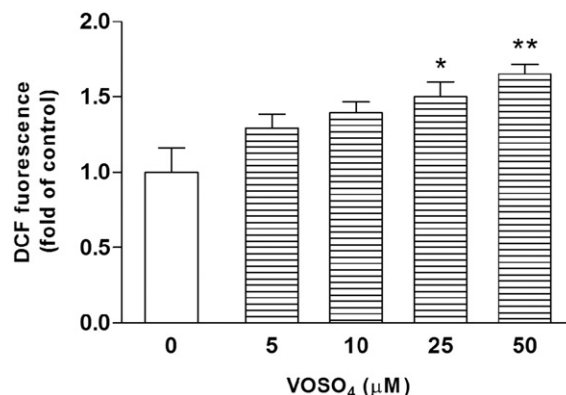


**Fig. 3.** Effects of VOSO<sub>4</sub> on ROS generation in HepG2 cells. HepG2 cells were exposed to 5, 10, 25 and 50  $\mu$ M VOSO<sub>4</sub> for 30 min. Intracellular ROS levels were determined by DCFH-DA staining. The fluorescence intensity of DCF was measured by fluorescence plate reader (TriStar LB 941). Data are presented as mean  $\pm$  SEM of three independent experiments. \* $p < 0.05$ , \*\* $p < 0.01$  vs. the untreated control cells. # $p < 0.05$  vs. VOSO<sub>4</sub>-treated cells.

### 3.4. VOSO<sub>4</sub> induces hydroxyl radicals generation

To further confirm whether  $\cdot\text{OH}$  radical was induced by VOSO<sub>4</sub>, the ability of VOSO<sub>4</sub> to generate  $\cdot\text{OH}$  radical was detected using an ESR spin trapping method with DMPO as the spin trap. The spectrum consists of a 1:2:2:1 quartet with a splitting of  $a_{\text{H}} = a_{\text{N}} = 14.9$  G, where  $a_{\text{N}}$  and  $a_{\text{H}}$  denote the hyperfine splitting of the nitroxyl nitrogen and  $\alpha$ -hydrogen, respectively. Based on these splittings and the 1:2:2:1 line shape, this spectrum was assigned to the DMPO/ $\cdot\text{OH}$  adduct, which was evidence of  $\cdot\text{OH}$  radical generation. As shown in Fig. 4, HepG2 cells alone did not generate any detectable amount of free radicals (Fig. 4A-1). However, the cells incubated with VOSO<sub>4</sub> generated a typical ESR spectrum (Fig. 4A-2). NADPH, a cofactor of

certain flavoenzymes such as glutathione reductase, slightly enhanced the generation of the  $\cdot\text{OH}$  radical (Fig. 4A-3). Neither DPI nor rotenone decreased the signal intensity induced by VOSO<sub>4</sub> (Fig. 4A-4, 5). Addition of SOD, an  $\text{O}_2^{\cdot-}$  radical scavenger, significantly increased the DMPO/ $\cdot\text{OH}$  adduct signal (Fig. 4A-6). However, addition of CAT, a scavenger of  $\text{H}_2\text{O}_2$ , inhibited  $\cdot\text{OH}$  radical generation (Fig. 4A-7), indicating that  $\text{H}_2\text{O}_2$  was produced in the VOSO<sub>4</sub>-treated cells and involved in  $\cdot\text{OH}$  generation. Addition of sodium formate, an  $\cdot\text{OH}$  radical scavenger, decreased the signal intensity (Fig. 4A-8), further supporting the  $\cdot\text{OH}$  radical generation. These results indicated that  $\cdot\text{OH}$  generation by VOSO<sub>4</sub> might be required for its stimulation of glucose uptake.

### 3.5. Requirement of hydroxyl radicals for induction of glucose uptake

To further study of the role of ROS in VOSO<sub>4</sub>-stimulated glucose uptake, the effects of various specific antioxidants on glucose uptake in HepG2 cells were determined. As shown in Fig. 5, treatment of the cells with VOSO<sub>4</sub> increased D-[U-<sup>14</sup>C]glucose uptake, and addition of CAT and sodium formate significantly decreased glucose uptake. In contrast, treatment of the cells with SOD did not significantly decrease glucose uptake induced by VOSO<sub>4</sub>.

### 3.6. Involvement of hydroxyl radicals in IR/Akt phosphorylation

To understand whether VOSO<sub>4</sub>-induced ROS generation play a role in VOSO<sub>4</sub>-stimulated glucose uptake through the IR/Akt pathway, the effects of various antioxidants on VOSO<sub>4</sub>-induced IR and Akt phosphorylation were determined by immunoblot assay. As shown in Fig. 6, treatment of the cells with 25  $\mu\text{M}$  VOSO<sub>4</sub> induced IR and Akt phosphorylation. CAT and sodium formate significantly inhibited VOSO<sub>4</sub>-induced IR and Akt phosphorylation. In contrast, treatment of the cells with SOD did not inhibit IR and Akt phosphorylation. These results further confirmed that  $\cdot\text{OH}$  as a signaling molecular was involved in VOSO<sub>4</sub>-induced IR/Akt phosphorylation.

## 4. Discussion

In this study, we have demonstrated that oxidovanadium(IV) sulfate improves glucose uptake in human hepatoma cell line HepG2. Further, we showed that VOSO<sub>4</sub>-induced  $\cdot\text{OH}$  radical serves as one of the metabolic signals for glucose uptake. Therefore, we assessed the underlying mechanism of VOSO<sub>4</sub> on glucose uptake. The increase in glucose uptake by VOSO<sub>4</sub> was predominantly mediated by activation of Akt activity. In addition, the IR/Akt is required for induction of central signaling pathway regulating cellular glucose uptake response to  $\cdot\text{OH}$  radical generation.

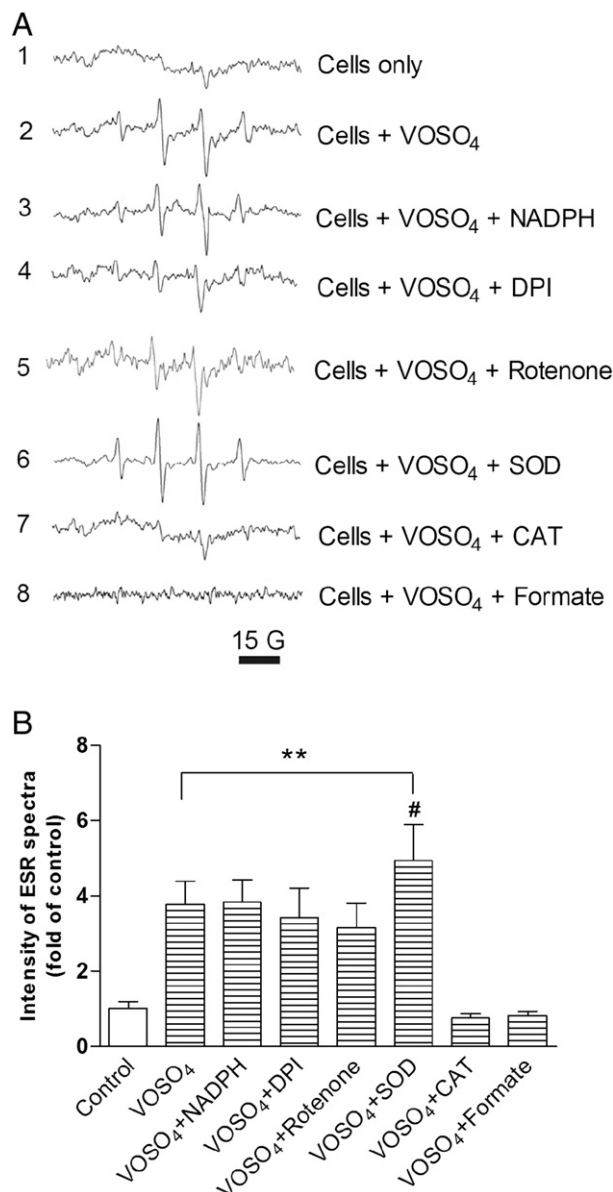


**Fig. 4.** Effects of antioxidants on VOSO<sub>4</sub>-induced ROS generation in HepG2 cells. HepG2 cells ( $1 \times 10^7$ ) were incubated in PBS containing 100 mM DMPO and 1 mM VOSO<sub>4</sub> with or without antioxidants, DPI, and rotenone. ESR spectra were recorded for 5 min. 1, HepG2 cells only; 2, cells + VOSO<sub>4</sub> (1 mM); 3, cells + VOSO<sub>4</sub> + NADPH (1 mM); 4, cells + VOSO<sub>4</sub> + DPI (20  $\mu\text{M}$ ); 5, cells + VOSO<sub>4</sub> + rotenone (50  $\mu\text{M}$ ); 6, cells + VOSO<sub>4</sub> + SOD (1000 U/ml); 7, cells + VOSO<sub>4</sub> + CAT (5000 U/ml); 8, cells + VOSO<sub>4</sub> + sodium formate (300  $\mu\text{M}$ ). A, The ESR spectra from a representative experiment. B, Data are presented as mean  $\pm$  SEM of three independent experiments (Control = 1). \*\* $p < 0.01$  vs. the untreated control cells. # $p < 0.05$  vs. VOSO<sub>4</sub>-treated cells.

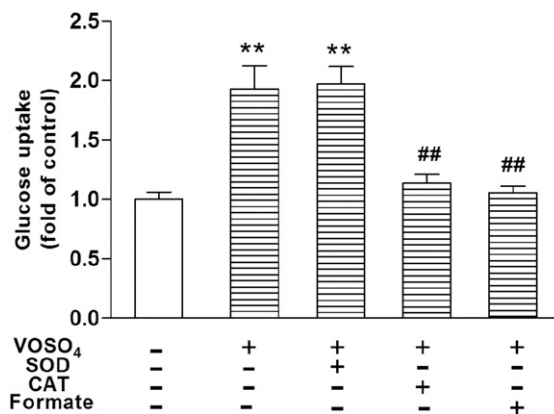


**Fig. 5.** Effects of antioxidants on VOSO<sub>4</sub>-induced glucose uptake in HepG2 cells. Cells were pretreated with 1000 U/ml SOD, 5000 U/ml CAT and with 300  $\mu\text{M}$  sodium formate, respectively. Then the cells were treated with 25  $\mu\text{M}$  VOSO<sub>4</sub> for 30 min. Glucose uptake in cells was determined. Data are presented as mean  $\pm$  SEM of three independent experiments. \*\* $p < 0.01$  vs. the untreated control cells. ## $p < 0.01$  vs. VOSO<sub>4</sub>-treated cells.



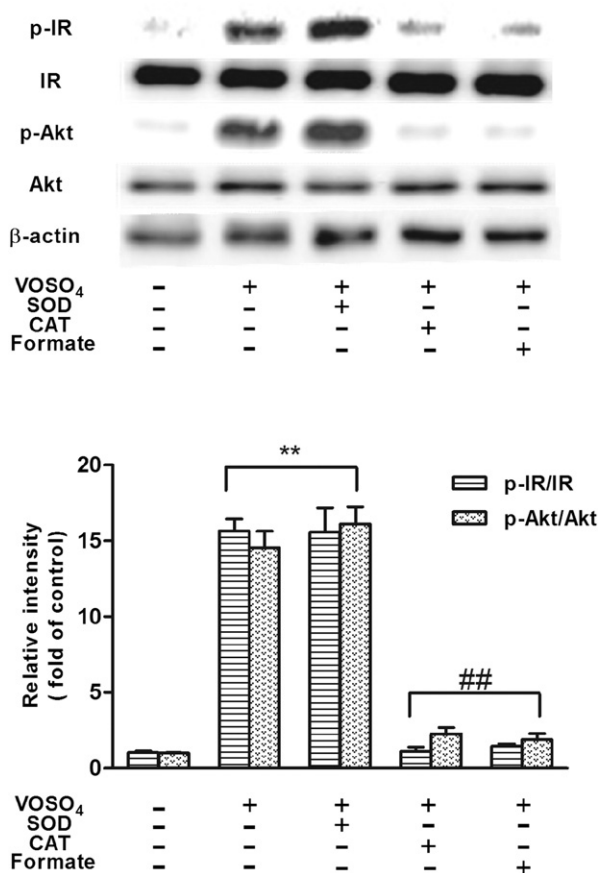


**Fig. 6.** Effects of antioxidants on VOSO<sub>4</sub>-induced IR and Akt phosphorylation in HepG2 cells. Cells were pretreated with 1000 U/ml SOD, 5000 U/ml CAT and 300 μM sodium formate, respectively. Then the cells were incubated with 25 μM VOSO<sub>4</sub> for 30 min. Immunoblotted with phospho-IR (Tyr942) and phospho-Akt (Ser473) antibodies to examine the phosphorylation status and subsequently immunoblotted with the anti-IR and anti-Akt antibodies as loading control. The phosphorylation density of the IR and Akt from replicate quantitated using ImageJ software was shown in the bar graph. The mean densitometry data from three independent experiments (one of which is shown here) were normalized to the result obtained in cells in the absence of VOSO<sub>4</sub> (control). Data are presented as mean ± SEM of three independent experiments. \*\*p < 0.01 vs. the untreated control cells. ##p < 0.01 vs. VOSO<sub>4</sub>-treated cells.

These data are consistent with the previous reports that vanadium appears to have a profound impact on insulin action through the insulin signaling cascade [12,36–38].

Tardif et al. described that vanadate induces a dose-dependent increase in glucose uptake in cardiomyocytes [39]. More recently, Hwang and Chang described that vanadium pentoxide stimulates glucose uptake in L6 myotubes [40]. Similarly, we also observed that VOSO<sub>4</sub> significantly increased the levels of glucose uptake in HepG2 cells in a dose-dependent manner (Fig. 1), suggesting the insulin signaling pathway activated by VOSO<sub>4</sub> treatment leading to enhanced glucose uptake. Activation of this cascade by VOSO<sub>4</sub> also induced a dose-dependent increase in glucose uptake in HepG2 cells. This observation is consistent with an earlier report demonstrating that the dose-dependent stimulation of glucose uptake in adipocytes was more sensitive to vanadate in cells rendered insulin-resistant by exposure to high glucose. The increased sensitivity of glucose uptake was paralleled by an increased sensitivity of IR phosphorylation and Tyr kinase activity [41].

Rehder described the ability of vanadium to regulate the cellular production of ROS [42]. Under physiological conditions and vanadium concentrations below 100 μM, vanadate is rapidly reduced to V<sup>IV</sup>O<sup>2+</sup> upon entering cells [43]. It has been demonstrated that VO<sup>2+</sup> is able to generate ·OH radical from hydrogen peroxide via a Fenton-like

reaction [42]. In the present study, we showed that VOSO<sub>4</sub> triggered an increase of intracellular ROS in a dose-dependent manner as determined by dye staining (Fig. 3). Also, ESR spin trapping measurements show that cells treated with VOSO<sub>4</sub> generated ·OH radical (Fig. 4A). Catalase and sodium formate, as a specific scavenger of H<sub>2</sub>O<sub>2</sub> or ·OH, dramatically decreased the generations of ROS and ·OH induced by VOSO<sub>4</sub> (Fig. 4B). These observations are consistent with the previous reports that incubation of cells with vanadium led to an increase in the generation of ROS [33,35,44,45].

Early studies have demonstrated that vanadium exposure induces intracellular ROS generation, which function as signaling species to activate calcium-calmodulin pathways in T cells [33] or to trigger p53 activation in A549 cells [34]. ROS clearly possess the capacity to behave in a random and can directly or indirectly activate cellular stress-sensitive signaling pathways [46]. It is well known that ROS generation is believed to be essential in triggering signaling response of insulin [47]. Previous studies have identified that the exposure of cells to ROS or ROS generating systems is capable of stimulating cellular Akt activity [48,49]. In line with this signal-stimulating effect of ROS, redox-active transition metal ions capable of generating ROS in cells were demonstrated to stimulate Akt also [26]. For example, exposure to Cu(II) salts triggers an activation of Akt in human and rat hepatoma cells and rat liver epithelial cells [28,50]. Orthovanadate results in increased phosphorylation of RET/PTC1 for Tyr451 and activation of the PI3K/Akt/mTOR signaling pathway [51]. In this present study, we also observed that VOSO<sub>4</sub>-induced ROS caused activation of IR and Akt (Fig. 2). Moreover, catalase and sodium formate significantly inhibited IR and Akt phosphorylation induced by VOSO<sub>4</sub> (Fig. 6), suggesting that ·OH is involved in VOSO<sub>4</sub>-induced IR and Akt phosphorylation.

Although ROS enhance insulin signaling, particularly, H<sub>2</sub>O<sub>2</sub> has been identified as a suitable second messenger molecule, excessive levels of ROS may cause diabetic complications [52]. Moreover, oxidative stress is believed to be the common denominator for the major pathways involved in the development and progression of diabetic diseases [53]. In the present study, we observed an increase of ROS generation that was significantly different from control levels, at 25 μM and 50 μM of VOSO<sub>4</sub> (Fig. 3). However, the maximum level of glucose uptake was reached at 25 μM of VOSO<sub>4</sub> (Fig. 1). Therefore, ROS generation needs to be closely monitored in applying vanadium compounds *in vitro* and *in vivo* due to the cytotoxic nature of ROS.

In conclusion, the present study demonstrated that VOSO<sub>4</sub>-induced ROS generation elicits glucose uptake in HepG2 cells. Moreover, our findings revealed an interaction between ROS generation and IR/Akt activation in VOSO<sub>4</sub>-treated cells. We found that VOSO<sub>4</sub>-induced ·OH radical, as the major species of ROS, is responsible for glucose uptake and IR/Akt phosphorylation. These results suggest that increase of glucose uptake induced by VOSO<sub>4</sub> through IR/Akt signaling pathway, ·OH radical may play an important role.

## Abbreviations

CAT	catalase
DCFH-DA	2',7'-dichlorodihydrofluorescein diacetate
DMPO	5,5-dimethyl-1-pyrroline-N-oxide
DPI	diphenylene iodonium
ECL	enhanced chemiluminescence
ESR	electron spin resonance
IR	insulin receptor
PEPCK	phosphoenolpyruvate carboxykinase
PI3K	phosphatidylinositol 3-kinase
PMSF	polymethylsulfonyl fluoride
PTPase	protein tyrosine phosphatase
PVDF	poly (vinylidene fluoride)
RIPA	radio immunoprecipitation assay
ROS	reactive oxygen species

SEM standard error of mean  
 SOD superoxide dismutase  
 TBST Tris-buffered saline (20 mM Tris-HCl and 150 mM NaCl, pH 7.4) containing 0.1% Tween 20

### Conflict of interest

All authors declare that there are no conflicts of interest.

### Acknowledgments

This work was supported by grants from the National Natural Science Foundation of China (Nos.11075207, 20871120).

### References

- [1] M. Li, J.J. Smee, W. Ding, D.C. Crans, J. Inorg. Biochem. 103 (2009) 585–589.
- [2] T.K. Saha, Y. Yoshikawa, H. Sakurai, J. Pharm. Pharmacol. 59 (2007) 437–444.
- [3] H. Sakurai, K. Tsuchiya, M. Nukatsuka, M. Sofue, J. Kawada, J. Endocrinol. 126 (1990) 451–459.
- [4] G.R. Willsky, L.H. Chi, Y. Liang, D.P. Gaile, Z. Hu, D.C. Crans, Physiol. Genomics 26 (2006) 192–201.
- [5] H. Degani, M. Gochin, S.J. Karlsh, Y. Shechter, Biochemistry 20 (1981) 5795–5799.
- [6] A. Green, Biochem. J. 238 (1986) 663–669.
- [7] Y. Shechter, I. Goldwasser, M. Mironchik, H. Tsubery, M. Fridkin, Pure Appl. Chem. 77 (2005) 1617–1628.
- [8] N. Sekar, J. Li, Z. He, D. Gefel, Y. Shechter, Endocrinology 140 (1999) 1125–1131.
- [9] T.A. Clark, A.L. Edel, C.E. Heyliger, G.N. Pierce, Can. J. Physiol. Pharmacol. 82 (2004) 888–894.
- [10] K.H. Thompson, C. Orvig, J. Inorg. Biochem. 100 (2006) 1925–1935.
- [11] I.A. Setyawati, K.H. Thompson, V.G. Yuen, Y. Sun, M. Battell, D.M. Lyster, C. Vo, T.J. Ruth, S. Zeisler, J.H. McNeill, C. Orvig, J. Appl. Physiol. 84 (1998) 569–575.
- [12] D. Wei, M. Li, W. Ding, J. Biol. Inorg. Chem. 12 (2007) 1265–1273.
- [13] F. Liu, M. Xie, D. Chen, J. Li, W. Ding, J. Diabetes Res. 2013 (2013) 956737.
- [14] M. Xie, D. Chen, F. Zhang, G.R. Willsky, D.C. Crans, W. Ding, J. Inorg. Biochem. 136 (2014) 47–56.
- [15] P. Buglyo, D.C. Crans, E.M. Nagy, R.L. Lindo, L. Yang, J.J. Smee, W. Jin, L.H. Chi, M.E. Godzala III, G.R. Willsky, Inorg. Chem. 44 (2005) 5416–5427.
- [16] M. Haratake, M. Fukunaga, M. Ono, M. Nakayama, J. Biol. Inorg. Chem. 10 (2005) 250–258.
- [17] M. Li, W. Ding, J.J. Smee, B. Baruah, G.R. Willsky, D.C. Crans, Biometals 22 (2009) 895–905.
- [18] B.R. Nechay, Annu. Rev. Pharmacol. Toxicol. 24 (1984) 501–524.
- [19] M. Yoshinaga, T. Ueki, N. Yamaguchi, K. Kamino, H. Michibata, Biochim. Biophys. Acta 1760 (2006) 495–503.
- [20] D. Rehder, Angew. Chem. Int. Ed. 30 (1991) 148–167.
- [21] C.K. Roberts, K.K. Sindhu, Life Sci. 84 (2009) 705–712.
- [22] V.L. Voelkov, Cell. Mol. Biol. 51 (2005) 663–675.
- [23] J. Ye, M. Ding, S.S. Leonard, V.A. Robinson, L. Millecchia, X. Zhang, V. Castranova, V. Vallyathan, X. Shi, Mol. Cell. Biochem. 202 (1999) 9–17.
- [24] J. Frijhoff, M. Dagnell, M. Augsten, E. Beltrami, M. Giorgio, A. Ostman, Free Radic. Biol. Med. 68 (2014) 268–277.
- [25] F.G. Meng, Z.Y. Zhang, Biochim. Biophys. Acta 1834 (2013) 464–469.
- [26] A. Eckers, L.O. Klotz, Redox Rep. 14 (2009) 141–146.
- [27] C.M. Taniguchi, B. Emanuelli, C.R. Kahn, Nat. Rev. Mol. Cell Biol. 7 (2006) 85–96.
- [28] P.L. Walter, A. Kampkotter, A. Eckers, A. Barthel, D. Schmoll, H. Sies, L.O. Klotz, Arch. Biochem. Biophys. 454 (2006) 107–113.
- [29] A. Tardif, N. Julien, A. Pelletier, G. Thibault, A.K. Srivastava, J.L. Chiasson, L. Coderre, Am. J. Physiol. Endocrinol. Metab. 281 (2001) E1205–E1212.
- [30] S. Jackson, S.M. Bagstaff, S. Lynn, S.J. Yeaman, D.M. Turnbull, M. Walker, Diabetes 49 (2000) 1169–1177.
- [31] C.P. LeBel, H. Ischiropoulos, S.C. Bondy, Chem. Res. Toxicol. 5 (1992) 227–231.
- [32] A. Gomes, E. Fernandes, J.L. Lima, J. Biochem. Biophys. Methods 65 (2005) 45–80.
- [33] C. Huang, M. Ding, J. Li, S.S. Leonard, Y. Rojanasakul, V. Castranova, V. Vallyathan, G. Ju, X. Shi, J. Biol. Chem. 276 (2001) 22397–22403.
- [34] X. Shi, N.S. Dalal, Free Radic. Res. Commun. 17 (1992) 369–376.
- [35] N. Gao, M. Ding, J.Z. Zheng, Z. Zhang, S.S. Leonard, K.J. Liu, X. Shi, B.H. Jiang, J. Biol. Chem. 277 (2002) 31963–31971.
- [36] D.W. Kwong, W.N. Leung, M. Xu, S.Q. Zhu, C.H. Cheng, J. Inorg. Biochem. 64 (1996) 163–180.
- [37] M. Li, W. Ding, B. Baruah, D.C. Crans, R. Wang, J. Inorg. Biochem. 102 (2008) 1846–1853.
- [38] N. Sekar, J. Li, Y. Shechter, Crit. Rev. Biochem. Mol. Biol. 31 (1996) 339–359.
- [39] A. Tardif, N. Julien, J.L. Chiasson, L. Coderre, Am. J. Physiol. Endocrinol. Metab. 284 (2003) E1055–E1064.
- [40] S.L. Hwang, H.W. Chang, Mol. Cell. Biochem. 360 (2012) 401–409.
- [41] B. Lu, D. Ennis, R. Lai, E. Bogdanovic, R. Nikolov, L. Salamon, C. Fantus, H. Le-Tien, I.G. Fantus, J. Biol. Chem. 276 (2001) 35589–35598.
- [42] D. Rehder, Dalton Trans. 42 (2013) 11749–11761.
- [43] L.A. Minasi, A. Chang, G.R. Willsky, J. Biol. Chem. 265 (1990) 14907–14910.
- [44] J. Rivadeneira, D.A. Barrio, G. Arrambide, D. Gambino, L. Bruzzone, S.B. Etcheverry, J. Inorg. Biochem. 103 (2009) 633–642.
- [45] G.R. Willsky, L.H. Chi, M. Godzala III, P.J. Kostyniak, J.J. Smee, A.M. Trujillo, J.A. Alfano, W. Ding, Z. Hu, D.C. Crans, Coord. Chem. Rev. 255 (2011) 2258–2269.
- [46] J. Fu, C.G. Woods, E. Yehuda-Shnaidman, Q. Zhang, V. Wong, S. Collins, G. Sun, M.E. Andersen, J. Pi, Environ. Health Perspect. 118 (2010) 864–870.
- [47] K. Mahadev, X. Wu, A. Zilbering, L. Zhu, J.T. Lawrence, B.J. Goldstein, J. Biol. Chem. 276 (2001) 48662–48669.
- [48] K. Abdelmohsen, P.A. Gerber, C. von Montfort, H. Sies, L.O. Klotz, J. Biol. Chem. 278 (2003) 38360–38367.
- [49] X. Wang, K.D. McCullough, T.F. Franke, N.J. Holbrook, J. Biol. Chem. 275 (2000) 14624–14631.
- [50] E.A. Ostrakhovitch, M.R. Lordnejad, F. Schliess, H. Sies, L.O. Klotz, Arch. Biochem. Biophys. 397 (2002) 232–239.
- [51] A.P. Goncalves, A. Videira, P. Soares, V. Maximo, Life Sci. 89 (2011) 371–377.
- [52] H. Sies, J. Biol. Chem. 289 (2014) 8735–8741.
- [53] L. Rochette, M. Zeller, Y. Cottin, C. Vergely, Biochim. Biophys. Acta 1840 (2014) 2709–2729.